Zigzag Graphene Nanoribbons and Confluent Supersymmetry

A Contreras-Astorga[1,2], L Hernandez-Martinez[3] and L G Toscano-Flores[4]

[1] CONACyT-Physics Department, Cinvestav, P.O. Box. 14-740, 07000 Mexico City, Mexico
[2] Canadian Quantum Research Center, 204-3002 32 Ave Vernon, BC V1T 2L7, Canada
[3] Institute of Physics, UNAM, P.O. Box. 20-364, 04510 Mexico City, Mexico
[4] Instituto Politécnico Nacional, Escuela Superior de Ingeniería y Arquitectura, Av. Miguel Bernard s/n, Adolfo López Mateos, Col. Zacatenco, C.P. 07738 Cd. de México, México

E-mail: alonso.contreras@conacyt.mx, luisj@estudiantes.fisica.unam.mx, ltoscanof@ipn.mx

Abstract. We studied the behavior of charge carriers in graphene nanoribbons with zigzag edges. We start from free nanoribbons, and by using second-order confluent supersymmetry, we added external magnetic fields perpendicular to the graphene layer. The technique allows us to obtain explicit expressions for the solution of the Dirac equation and gives the transcendental equations that must be solved to obtain the energy spectrum.

1. Introduction

Graphene is a single layer of honeycomb arranged atoms of carbon, this two-dimensional structure can be rolled to form nanotubes, can be bent to form fullerenes, or it can also be stacked to form graphite. Although it was theoretically described in 1947 [1], it was found in the laboratory until 2004 by Novoselov et al. [2]. Graphene has a variety of interesting electric properties, which makes it a good candidate to take the place of traditional semiconductor materials in an attempt to reduce the size of electronic components. It also is an excellent subject of study per se because its charge carriers are ruled by the Dirac equation instead of by the Schrödinger equation as in conventional condensed matter materials [3, 4].

At low energies, $|\epsilon^{\pm}| < 2$ eV, the electron dispersion relation is linear $\epsilon^{\pm}(\boldsymbol{k}) = \pm\hbar v_F|\boldsymbol{k}|$, where $v_F \sim c/300$ is the Fermi velocity [4]. The Hamiltonian ruling the excitations is recovered using the prescription $\boldsymbol{p} \to \boldsymbol{\sigma}\cdot\boldsymbol{p}$, i.e. $H = v_F\boldsymbol{\sigma}\cdot\boldsymbol{p}$, where $\boldsymbol{\sigma} = (\sigma_x, \sigma_y)$ is a vector with Pauli matrices and $\boldsymbol{p} = -i\hbar(\partial_x, \partial_y)$ is the two-dimensional momentum operator. The explicit form of the Dirac equation becomes

$$v_F(\boldsymbol{\sigma}\cdot\boldsymbol{p})\Psi(x,y) = \epsilon\Psi(x,y), \tag{1}$$

Here, Ψ is a two entry spinor $\Psi(x,y) = (\psi^{(A)}(x,y), \psi^{(B)}(x,y))^T$. To introduce the interaction with a perpendicular magnetic field $\boldsymbol{B} = B(x,y)\hat{e}_z = \nabla\times\boldsymbol{A}$ we make the substitution $\boldsymbol{p} \to \boldsymbol{p} + e\boldsymbol{A}/c$ in the Hamiltonian.

A graphene nanoribbon consists of a thin band of graphene; depending on the orientation of the carbon atoms at the edges of the ribbon will have different terminations. If the edges coincide

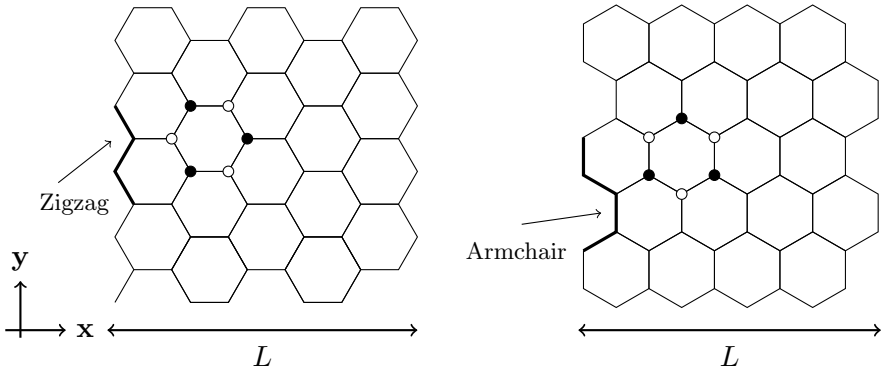

(a) Zigzag edges. (b) Armchair edges.

Figure 1. Portion of a graphene nanoribbon of width L with zigzag edges (a) and armchair edges (b). Black and white dots represent the triangular sublattices of graphene.

with the Bravais lattice vectors, the ribbon will be named 'zigzag ribbon'. If instead, the edges coincide with the parallel sides of the hexagon formed by the atoms, then the ribbon will be known as 'armchair ribbon', as seen in Figure 1; here, the edges of the ribbon are represented vertically, and the width horizontally. It is relevant to determine the type of ribbon to study because the electronic properties will depend on the band's size and geometry and the boundary conditions [5].

Electromagnetic fields can be applied to modify the behavior of charge carriers in graphene. Different effects can be studied in this two-dimensional material as the Hall effect or Klein tunneling [6, 7]. Supersymmetric quantum mechanics (susy) is a technique used to find exact solutions to the Dirac equation with electromagnetic fields [8–12]. This technique maps solutions of an eigenvalue equation into solutions of a new eigenvalue equation. In this work, we show how to apply an iteration of this method, known as confluent supersymmetry, to zigzag nanoribbons. In other words, we map solutions of the Dirac equation associated with free zigzag nanoribbons into the case of a position-dependent magnetic field.

This paper is organized as follows: In Section 2, we present the initial system, free zigzag graphene nanoribbons, its particular boundary conditions, the solutions of the Dirac equation, and its spectrum. In Section 3, we present a summary of confluent supersymmetry applied to Schrödinger equations. The main results of this work are in Section 4, where we present exact solutions of the Dirac equation for zigzag nanoribbons under a perpendicular magnetic field. We finalize with our conclusions.

2. Free zigzag graphene nanoribbons

The study of solutions to the Dirac equation for graphene nanoribbons was originally done by Brey and Fertig [5, 13]. While the particular boundary conditions of nanoribbons are discussed in [14, 15], a more complete discussion is given by Castro Neto in [4]. Our subject of study is a graphene nanoribbon (GNR) of finite width $L = 1$ and infinite length, with zigzag edges at $x = 0$ and $x = 1$, in order to simplify notation we use units where $\hbar = v_F = 1$. The translational symmetry of the system allows us to separate variables using $\Psi_n(x, y) =$

$e^{ik_y y}\,\Phi_n(x) = e^{ik_y y}\,(\phi_n^{(A)}(x), \phi_n^{(B)}(x))^T$. Then, the Dirac equation reads

$$\begin{pmatrix} 0 & -i\frac{d}{dx} - i\,k_y \\ -i\frac{d}{dx} + i\,k_y & 0 \end{pmatrix} \begin{pmatrix} \phi_n^{(A)}(x) \\ \phi_n^{(B)}(x) \end{pmatrix} = \epsilon_n \begin{pmatrix} \phi_n^{(A)}(x) \\ \phi_n^{(B)}(x) \end{pmatrix}. \tag{2}$$

Equivalently, we can write the system of coupled equations

$$\phi_n^{(A)}(x) = \frac{-i}{\epsilon_n}\left(\frac{d}{dx} + k_y\right)\phi_n^{(B)}(x), \tag{3}$$

$$\phi_n^{(B)}(x) = \frac{i}{\epsilon_n}\left(-\frac{d}{dx} + k_y\right)\phi_n^{(A)}(x). \tag{4}$$

We can decouple the first component by substituting (4) into (3), then $\phi_n^{(A)}$ satisfies the Schrödinger equation

$$-\phi_n^{\prime\prime(A)}(x) + k_y^2\,\phi_n^{(A)}(x) = \epsilon_n^2\,\phi_n^{(A)}(x), \tag{5}$$

with general solution

$$\phi_n^{(A)}(x) = \alpha\, e^{z_n\, x} + \beta\, e^{-z_n\, x}, \tag{6}$$

where $z_n^2 = k_y^2 - \epsilon_n^2$. The second component of the spinor $\phi_n^{(B)}(x)$ is directly obtained using (4). The zigzag geometry of the edges imposes the following boundary conditions

$$\phi_n^{(A)}(0) = \phi_n^{(B)}(1) = 0. \tag{7}$$

The second boundary condition, $\phi_n^{(B)}(1) = 0$, gives us a transcendental equation for z_n a real value

$$e^{-2\,z_n} = \frac{k_y - z_n}{k_y + z_n}, \tag{8}$$

and a different transcendental equation for $z_n = ik_n$ a pure imaginary value

$$\tan k_n = \frac{k_n}{k_y}. \tag{9}$$

Each solution of z_n from (8) and k_n from (9) gives us an energy eigenvalue ϵ_n of the spectrum of the Dirac Hamiltonian H. There is an important example, studied by Brey and Ferting [5], when $k_y = 0$ then $z_n = ik_n$ is a pure imaginary number, by solving (9) the energy spectrum is $\epsilon_n = \pm(2n+1)\pi/2$, and the spinor components have the expressions

$$\phi_n^{(A)}(x) = 2\,i\alpha\,\sin k_n\, x, \qquad \phi_n^{(B)}(x) = \frac{2\,\alpha}{\bar{\epsilon}}\,(k_n\,\cos k_n\, x - k_y \sin k_n\, x)\,, \tag{10}$$

where α is a normalization constant.

3. Confluent supersymmetry of the Schrödinger equation

Confluent supersymmetry is a higher-order susy transformation. There are different approaches leading to this transformation, here we present the main results with the formalism of Jordan chains as presented in [16]. In this work we will focus on second-order confluent supersymmetry. For different approaches consult [17–21]. It is worth noticing that there are matrix approaches that can be applied directly to Dirac equations, see for example [22, 23].

We start considering that the solution of the stationary Schrödinger equation is known

$$\phi'' + (E - V_0)\phi = 0, \tag{11}$$

where E is a real parameter and $V_0 = V_0(x)$ is the potential. Moreover, there are two functions $u_1,\ u_2$ that can be obtained by solving the system

$$u_1'' + (\lambda - V_0)u_1 = 0; \qquad u_2'' + (\lambda - V_0)u_2 = -u_1; \tag{12}$$

where λ is a real constant, the system (12) is a second-order Jordan chain and the functions $u_1,\ u_2$ are often referred as seed solutions or transformation functions. Note that u_1 is a particular solution of (11). Because u_1 solves a differential equation of second order, the Schrödinger equation, there must exist a second linearly independent solution $u_1^{\perp}$. The function $u_1^{\perp}$ must satisfy $W_{u_1,u_1^{\perp}} = 1$, where $W_{f,g}$ is the Wronskian of the functions indicated as indices. Then, $u_1^{\perp}$ can be written as

$$u_1^{\perp} = u_1 \int^x \frac{1}{u_1^2} dt. \tag{13}$$

The function u_2 can be found using the reduction of order formula and can be expressed in terms of u_1 and $u_1^{\perp}$ as

$$u_2 = u_1 + C\ u_1^{\perp} + u_1 \int^x \left(\int^t u_1^2 ds \right) \frac{1}{u_1^2} dt. \tag{14}$$

From the Jordan chain we can derive an useful property. First, we notice $W'_{u_1,u_2} = u_1 u_2'' - u_1'' u_2 = -u_1^2$, then integrating

$$W_{u_1,u_2} = \omega_0 - \int^x u_1^2 dt, \tag{15}$$

where ω_0 is an integration constant.

Once we determine the transformation functions u_1 and u_2, we can construct the function

$$\psi = \frac{W_{u_1,u_2,\phi}}{W_{u_1,u_2}} = \frac{W_{u_1,u_2,\phi}}{\omega_0 - \int^x u_1^2 dt}, \tag{16}$$

which is valid when $\lambda \neq E$. We can simplify further the last expression using (11), (12), and (15):

$$\psi = -\frac{W'_{u_1,u_2}}{W_{u_1,u_2}}\phi' + \left[(\lambda - E) - \frac{u_1 u_1'}{W_{u_1,u_2}} \right] \phi = \frac{u_1^2}{\omega_0 - \int^x u_1^2 dt}\phi' + \left[(\lambda - E) - \frac{u_1 u_1'}{\omega_0 - \int^x u_1^2 dt} \right] \phi. \tag{17}$$

This function satisfies the Schrödinger equation

$$\psi'' + (E - V_2)\psi = 0 \tag{18}$$

where V_2 is the confluent susy partner potential of V_0 and is given by

$$V_2 = V_0 - 2\frac{d^2}{dx^2} \ln W_{u_1,u_2} = V_0 + 2\frac{d}{dx} \left(\frac{u_1^2}{\omega_0 - \int^x u_1^2 dt} \right). \tag{19}$$

The degenerated case $\lambda = E$ needs more attention. Equation (16) reminds valid, but now the function ϕ must be taken as a linear combination of u_1 and $u_1^{\perp}$, then after some elementary row operations in the numerator Wronskian and using the Jordan chain, ψ takes the form

$$\psi = \frac{u_1}{W_{u_1,u_2}} = \frac{u_1}{\omega_0 - \int^x u_1^2 dt}. \tag{20}$$

It is worth noting that ω_0 and u_1 must be chosen so the Wronskian $W_{u_1,u_2} = \omega_0 - \int^x u_1^2 dt$ is a nodeless function in the domain of V_0 in order to generate a regular potential V_2.

4. Zigzag nanoribbons under magnetic fields

To analyze the problem of a zigzag nanoribbon under a perpendicular magnetic field, let us chose the Landau gauge $\mathbf{A}\,(x) = A_y(x)\,\hat{e}_y$ that generates the magnetic field $\mathbf{B} = \frac{d}{dx}\,A_y(x)\hat{e}_z$. Then the Dirac equation after separation of variables becomes

$$H\Phi(x) = \left(-i\sigma_x\frac{d}{dx} + \sigma_y\,\omega(x)\right)\,\Phi(x) = \epsilon_n\Phi(x), \tag{21}$$

where $\omega(x) = k_y + A_y(x)$. Again we used the spinor $\Phi_n(x) = \left(\phi_n^{(A)}(x), \phi_n^{(B)}(x)\right)^T$. As in Section 2, equation (21) can be written as two coupled equations. After decoupling, the upper component $\phi_n^{(A)}$ must satisfy

$$-\phi_n^{''(A)}(x) + V_0(x)\,\phi_n^{(A)}(x) = E_n\,\phi_n^{(A)}(x), \tag{22}$$

with potential $V_0(x) = \omega'(x) + \omega^2(x)$. Note that ϵ_n is the energy spectrum of Dirac Hamiltonian (21) while $E_n = \epsilon_n^2$ is the energy parameter in the Schrödinger equation (22).

4.1. Application of the confluent supersymmetry

Let us now apply the confluent susy algorithm, we start with the solution of the first equation of the Jordan chain (12) with a constant potential, as in the free zigzag nanoribbons (5):

$$u_1''(x) + \left(\lambda - k_y^2\right)\,u_1(x) = 0, \tag{23}$$

the domain of the potential being $x \in [0, 1]$. There are three possible scenarios for the seed solution u_1:

(i) If $\lambda < k_y^2$, then $u_1(x) = \cosh\left(\sqrt{k_y^2 - \lambda}\,x + \delta\right)$ where δ is a real constant.

(ii) If $\lambda = k_y^2$, then $u_1(x) = x + u_0$ with u_0 an integration constant.

(iii) If $\lambda > k_y^2$, the solution is $u_1(x) = \cos\left(\sqrt{\lambda - k_y^2}\,x + \delta\right)$ where $\delta \in [0, 2\pi)$ is a phase.

Once the seed solution is chosen, we can fix u_2 and the Wronskian $W_{u_1,u_2} = \omega_0 - \int^x u_1^2 dt$. Then, it is possible to construct a second Schrödinger equation

$$\phi_n^{(A,2)''} + (E - V_2)\phi_n^{(A,2)} = 0, \tag{24}$$

similar to (22) but with a potential V_2 given by (19). The solutions $\phi_n^{(A,2)}$ are constructed as in (16) from solutions $\phi_n^{(A)}$. An important remark is that we can shift the energy by a constant λ_2 as $\phi_n^{''(A,2)} + (E - \lambda_2 - \widetilde{V}_2)\phi_n^{(A,2)} = 0$, where $\widetilde{V}_2 = V_2 - \lambda_2$, this shift will be important later.

A Dirac Hamiltonian $H_2 = -i\sigma_x\,\frac{d}{dx} + \sigma_y\,\omega_2(x)$ can be constructed as in (21) looking for a function ω_2 related to the potential $\widetilde{V}_2$ as $\widetilde{V}_2 = \omega_2' + \omega_2^2$. With the ansatz

$$\omega_2(x) = \frac{d}{dx}\ln\nu(x) = \frac{\nu'(x)}{\nu(x)} \tag{25}$$

the Riccati equation transforms as

$$-\nu'' + V_2\,\nu = \lambda_2\nu. \tag{26}$$

Since this equation is the same Schrödinger equation as (24), there must be a function ν_0 solving (22) where $E = \lambda_2$ such that $\nu = W_{u_1,u_2,\nu_0}/W_{u_1,u_2}$. There are three possible solutions:

- If $\lambda_2 < k_y^2$ then $\nu_0 = \sinh\left(\sqrt{k_y^2 - \lambda_2}\, x + \beta\right)$.
- For $\lambda_2 = k_y^2$, $\nu_0 = x + r_0$ with r_0 an integration constant.
- Last case is $\lambda_2 > k_y^2$ and has the solution $\nu_0(x) = \sin\left(\sqrt{\lambda_2 - k_y^2}\, x + \beta\right)$.

The magnetic field associated with ω_2 is

$$\mathbf{B}_2(x) = \frac{d\,\omega_2(x)}{dx}\,\hat{e}_z \tag{27}$$

The spinor component $\phi_n^{(B,2)}(x)$ is obtained with the relation

$$\phi_n^{(B,2)}(x) = \frac{i}{\epsilon_{(2,n)}}\left[-\frac{d\,\phi_n^{(A,2)}(x)}{dx} + \omega_2(x)\,\phi_n^{(A,2)}(x)\right]. \tag{28}$$

The boundary conditions (7) must be satisfied by $\phi_n^{(A,2)}(x)$ and $\phi_n^{(B,2)}(x)$. They allow us to obtain the energies $\epsilon_{(2,n)}$. To fulfill the condition $\phi_n^{(A,2)}(0) = 0$ is sufficient to choose a seed function $u_1(0) = 0$, while the condition $\phi_n^{(B,2)}(1) = 0$ gives two transcendental equations to be solved:

$$\tanh z_n = \zeta(z_n) = -z_n\,\frac{g(1) - \omega_2(1)f(1) + f'(1)}{z_n^2 f(1) - g(1)\omega_2(1) + g'(1)}, \tag{29}$$

$$\tan k_n = \kappa(k_n) = k_n\,\frac{g(1) + f'(1) - \omega_2(1)f(1)}{k_n^2 f(1) + g(1)\omega_2(1) - g'(1)}. \tag{30}$$

where we used the abbreviations

$$f(x) = \frac{u_1^2}{\omega_0 - \int^x u_1^2 dt}, \qquad g(x) = \left[(\lambda - E) - \frac{u_1 u_1'}{\omega_0 - \int^x u_1^2 dt}\right], \tag{31}$$

4.2. Examples

In the next subsections we give explicit examples of zigzag nanoribbons under perpendicular magnetic fields.

4.2.1. Example 1, $\lambda > k_y^2 = 4$. Here we choose a seed solution u_1 and an auxiliary function ν_0 in the following way:

$$u_1(x) = \sin\left(\sqrt{\lambda - k_y^2}\, x\right), \quad \nu_0(x) = \sinh\left(\sqrt{k_y^2 - \lambda_2}\, x + \beta\right). \tag{32}$$

and the parameters $\lambda = 8,\ \lambda_2 = 3,\ \beta = 10$, and $\omega_0 = -2$.

The spinor component has two expressions, one when z_n is a real number

$$\phi_n^{(A,2)}(x) = -z_n\, f(x)\cosh z_n x + g(x)\sinh z_n x, \tag{33}$$

and another when $z_n = ik_n$ is a pure imaginary number

$$\phi_n^{(A,2)}(x) = -k_n\, f(x)\cos k_n x + g(x)\sin k_n x. \tag{34}$$

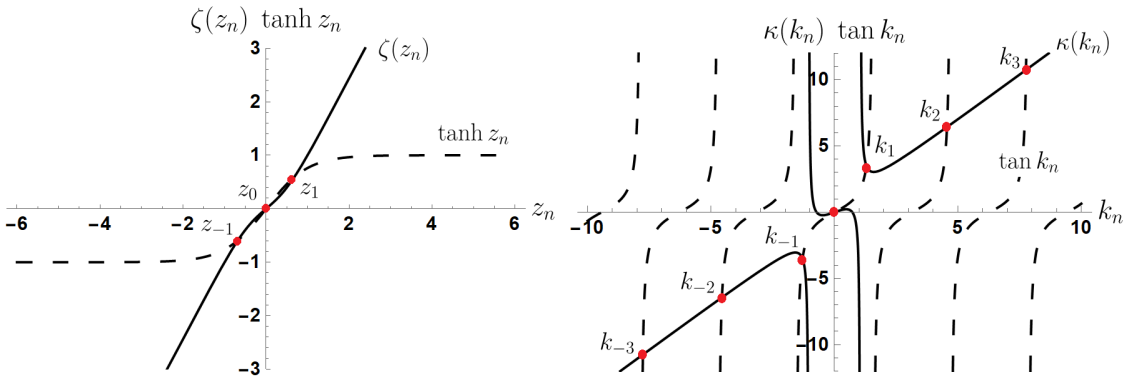

(a) Solutions for z_n a real number. (b) Solutions for $z_n = ik_n$.

Figure 2. Solution to the transcendental equations. Dots mark the intersection between the functions $\zeta(z_n)$ and $\tanh z_n$ of (29) and the functions $\kappa(k_n)$ and $\tan k_n$ of (30) for Example 1.

Recall that the functions $f(x)$ and $g(x)$ are defined in (31). The function $u_1(x)$ is null at $x = 0$ and, as a consequence, $f(0) = 0$. This ensures that the boundary condition $\phi_n^{(A,2)}(0) = 0$ is fulfilled. The second boundary condition $\phi_n^{(B,2)}(1) = 0$ imposes the transcendental equations (29) and (30) whose solutions are shown for the first n-values in Figure 2. The first eigenvalues are

$$|\epsilon_0| = 1.881, \quad |\epsilon_1| = 2.381, \quad |\epsilon_2| = 4.978, \quad |\epsilon_3| = 8.015. \tag{35}$$

The magnetic field and the components spinor for the lowest energy are plotted in Figure 3 (a) and (b) respectively.

4.2.2. Example 2, $\lambda = \lambda_2 = k_y^2 = 4$. This case is interesting because both function $u_1(x)$ and $\nu_0(x)$ are straight lines. We choose

$$u_1(x) = x, \qquad \nu_0(x) = x + 10, \tag{36}$$

and $\omega_0 = -2$. The condition $\phi_n^{(A,2)}(0) = 0$ is satisfied. The magnetic field in these conditions has a singularity at $x = 0$ because $\nu_0''(x) = 0$. Thus, $\nu(0) = 0$ and $\lim_{x\to 0} \omega_2(x) \to \infty$. However, the system has bound states. The first three eigenvalues of the Dirac equation are

$$|\epsilon_0| = 4.918, \quad |\epsilon_1| = 7.980, \quad |\epsilon_2| = 11.086. \tag{37}$$

The magnetic field and the components of the spinor for the lowest energy are shown in Figure 3 (a) and (c), respectively.

5. Conclusions

We studied zigzag graphene nanoribbons in the presence of external magnetic fields and found the eigenvalues and eigenfunctions of the corresponding Dirac equation. We use the confluent supersymmetry algorithm to generate the magnetic fields. We gave explicit expressions for each component of the eigenspinor. Due to the specific boundary conditions for zigzag terminations in graphene, it was necessary to solve a couple of transcendental equations numerically to find the eigenvalues. Finally, we presented two examples, one with a finite magnetic field and another field diverging at one of the edges. As a continuation of the present work, it would be interesting to compare our results with a numerical tight-binding calculation; moreover, it could be attractive to study slight perturbations of an external constant magnetic field in such nanoribbons.

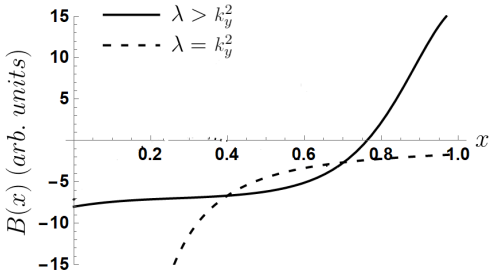

(a) Magnetic fields of Examples 1 and 2.

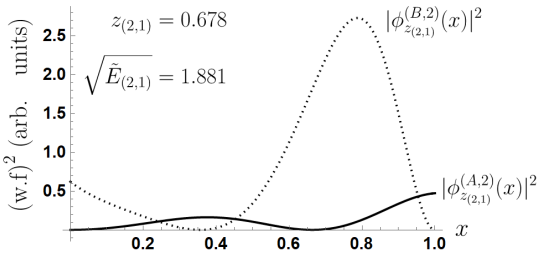

(b) Example 1, $\lambda > k_y^2 = 4$.

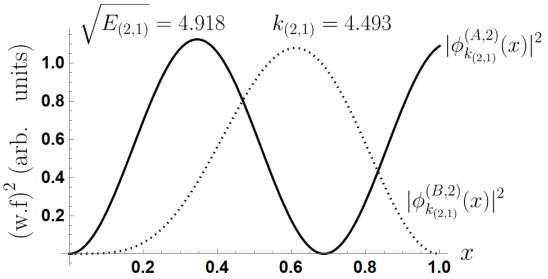

(c) Example 2, $\lambda = \lambda_2 = k_y^2 = 4$.

Figure 3. Magnetic fields of both examples (a) and the square of the normalized spinor components, $\phi_n^{(A,2)}(x)$ and $\phi_n^{(B,2)}(x)$, for each example (b) and (c) for the lowest energy level.

Acknowledgments
The authors acknowledge the support of CONACyT, grant FORDECYT-PRONACES/61533/2020.

References

[1] Wallace P R 1947 *Physical Review* **71** 622–634
[2] Novoselov K S, Geim A K, Morozov S V, Jiang D, Zhang Y, Dubonos S V, Grigorieva I V and Firsov A A 2004 *Science* **306** 666–669
[3] Geim A K and Novoselov K S 2007 *Nature Materials* **6** 183–191
[4] Castro Neto A H, Guinea F, Peres N M R, Novoselov K S and Geim A K 2009 *Reviews of Modern Physics* **81** 109–162
[5] Brey L and Fertig H A 2006 *Physical Review B* **73**(23) 235411
[6] Novoselov K S, Geim A K, Morozov S V, Jiang D, Katsnelson M I, Grigorieva I V, Dubonos S V and Firsov A A 2005 *Nature* **438** 197–200
[7] Katsnelson M I, Novoselov K S and Geim A K 2006 *Nature Physics* **2** 620–625
[8] Kuru S, Negro J and Nieto L M 2009 *Journal of Physics: Condensed Matter* **21** 455305
[9] Schulze-Halberg A and Roy B 2014 *Annals of Physics* **349** 159–170
[10] Midya B and Fernández C D J 2014 *Journal of Physics A: Mathematical and Theoretical* **47** 285302
[11] Castillo-Celeita M and Fernández C D J 2020 *Journal of Physics A: Mathematical and Theoretical* **53** 035302
[12] Jakubský V, Kuru S and Negro J 2022 *Physical Review B* **105** 165404
[13] Brey L and Fertig H A 2006 *Physical Review B* **73**(19) 195408
[14] Akhmerov A R and Beenakker C W J 2008 *Physical Review B* **77** 085423
[15] Freitas P and Siegl P 2014 *Reviews in Mathematical Physics* **26**
[16] Contreras-Astorga A and Schulze-Halberg A 2014 *Journal of Mathematical Physics* **55** 103506
[17] Baye D 1993 *Physical Review A* **48** 2040–2047
[18] Stahlhofen A A 1995 *Physical Review A* **51** 934–943
[19] Mielnik B, Nieto L and Rosas–Ortiz O 2000 *Physics Letters A* **269** 70–78
[20] Fernández C D J and Fernández-García N 2004 Higher-order supersymmetric quantum mechanics *AIP Conference Proceedings* vol 744 (AIP) pp 236–273 ISSN 0094243X
[21] Bermudez D, Fernández C D J and Fernández-García N 2012 *Physics Letters A* **376** 692–696

[22] Nieto L, Pecheritsin A and Samsonov B F 2003 *Annals of Physics* **305** 151–189
[23] Correa F and Jakubský V 2017 *Physical Review A* **95** 033807